

LoopSR: Looping Sim-and-Real for Lifelong Policy Adaptation of Legged Robots

Peilin Wu¹, Weiji Xie¹, Jiahang Cao¹, Hang Lai¹, and Weinan Zhang¹

Abstract—Reinforcement Learning (RL) has shown its remarkable and generalizable capability in legged locomotion through sim-to-real transfer. However, while adaptive methods like domain randomization are expected to make policy more robust to diverse environments, such comprehensiveness potentially detracts from the policy’s performance in any specific environment according to the No Free Lunch theorem, leading to a suboptimal solution once deployed in the real world. To address this issue, we propose a lifelong policy adaptation framework named LoopSR, which utilizes a transformer-based encoder to project real-world trajectories into a latent space, and accordingly reconstruct the real-world environments back in simulation for further improvement. Autoencoder architecture and contrastive learning methods are adopted to better extract the characteristics of real-world dynamics. The simulation parameters for continual training are derived by combining predicted parameters from the decoder with retrieved parameters from the simulation trajectory dataset. By leveraging the continual training, LoopSR achieves superior data efficiency compared with strong baselines, with only a limited amount of data to yield eminent performance in both sim-to-sim and sim-to-real experiments.

I. INTRODUCTION

Reinforcement Learning (RL) has seen significant progress as a viable alternative for robotic control, but applying it to real-world scenarios remains challenging. Advances in simulation systems [1, 2] and extensive parallel training [3] have enhanced policy performance and robustness, but the sim-to-real gap persists. Adaptive methods such as domain randomization [4–8] are widely used to address the gap and improve robustness. However, given RL methods’ inherent requirement of direct interaction with the environment, and along with No Free Lunch Theorem [9, 10], which suggests a potential trade-off between generalization and specific performance, purely training in the simulation with inaccurate state occupancy distribution will limit the policy’s performance beforehand.

Leveraging the data in the real world where the robot is directly situated is an intuitive solution to such a defect. Nevertheless, it still faces obstacles. Firstly, collecting real-world data is notoriously expensive while RL methods are extremely data-hungry. An applicable policy generally requires several months of real-world experience which is hardly affordable. Secondly, privileged knowledge (i.e. heightfield, contact force, mass, friction, etc) is absent in real-world settings, causing troubles when facing tricky terrains. One example is the stairs, where a blind robot with only proprioceptive observations (i.e. joint position & velocity) needs extensive exploration to learn to lift its legs. while the

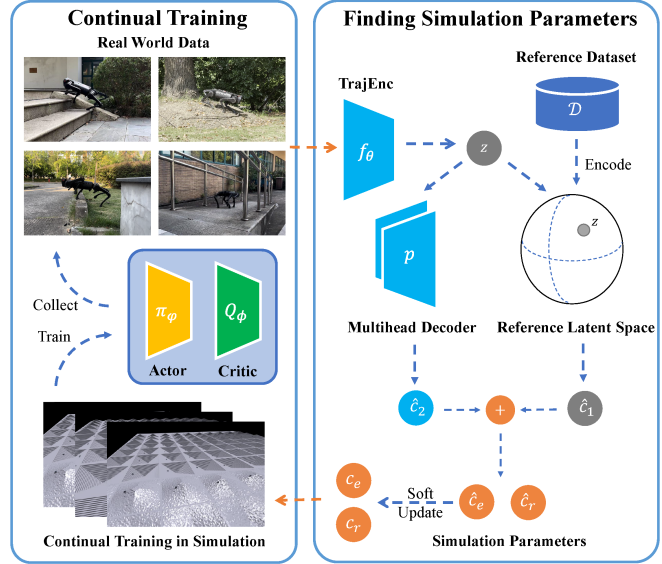


Fig. 1. Overview of our proposed LoopSR.

one with precise height information can better find such a solution. On top of that, noisy observation of the real world leads to training instability.

Previous works have attempted to cope with these impediments by reshaping reward functions [11, 12], taking advantage of sample-efficient algorithms [11–13], or harnessing model-based RL [14]. However, these existing methods, trained directly in the real world, fail to generate superior locomotion policies with safe and steady performance compared with prevailing zero-shot methods and are vulnerable in training.

Drawing intuition from the cognitive process where animals tend to leverage the experience in familiar environments when encountering new ones, we investigate to find a bridge back to the controllable simulation environment instead of trapping ourselves in the capricious and noisy real world. The benefits of such an idea are all-round. In one way, we can sidestep the bothering problem of redesigning a delicate reward function corresponding to the limited observation, and take full advantage of a well-polished simulation training process [1, 3, 4, 15, 16]. Additionally, with such a method, we only require a minimal amount of data to identify the surroundings well and still live off the benefits of data abundance in the simulation.

In this work, we present LoopSR, an effective pipeline for lifelong policy adaptation of legged robots depicted in Fig. 1. The core of LoopSR is a transformer-based encoder [17] to leverage the latent space. Particularly, we adopt autoencoder architecture [18, 19] and contrastive loss [20–25] to guide the

¹Dept. of Computer Sci. and Eng., Shanghai Jiao Tong University, China

model to extract sufficient features pertinent to reconstructing the simulation, ensuring the effectiveness and generalizability of the latent space. We implement both learning-based and retrieval-based methods to derive simulation parameters from the latent variable, which compensate for each other in accuracy and robustness to out-of-distribution scenes. LoopSR is tested in both IsaacGym simulated environment [1] and the real-world scene compared with strong baselines.

In a nutshell, the contributions of this paper can be summarized as follows:

- We proposed a novel lifelong policy adaptation method LoopSR that first incorporates real-world continual learning into simulated policy pretraining, achieving constant improvement during real-world deployments.
- We propose a representation-learning approach and construct an all-encompassing latent space for unlabeled trajectories. With the innovative combination of learning-based and retrieval-based methods, we successfully identify and rebuild the real world in simulation.
- We empirically validate LoopSR in both simulation and real-world environments. The results demonstrate the prominence of LoopSR compared with previous works.

II. RELATED WORKS

A. Representation Learning in RL

Representation learning [19, 26–28] has made up the bedrock for modern deep learning algorithms, and the field of RL and control is no exception. Previous works have made versatile attempts to take advantage of the representation learning and latent space [29–31], including contrastive learning [25, 32], reward function encoding [33, 34], domain/task-specific representation [18, 35–37], and gait encodings [38, 39], boosting multi-modal input [27] or transferring through different tasks and embodiment [36].

Typically, the domain representation is widely utilized for the task of meta-RL and transfer learning [40, 41]. However, real-world scenarios present a challenge as goal reward functions are not readily available, where we are obliged to focus on learning the representation of the transitions themselves rather than relying on labeled tasks.

B. Learning in the Real World

Continual learning in RL [42] is a daunting task as the result of the compounding error in drifted distribution. Works have been done to debase the trouble caused by protean data distribution through experience replay [43, 44], distillation [45], and reusing parts of model [46], etc. However, when it comes to real-world learning, the situation becomes progressively difficult due to noisy input, limited observation, and inaccessible reward functions.

[11–13] are among the few works tapping into this tricky problem. Instead of sim-to-real transfer, Smith et al. have decided to completely learn the policy in the real world, and have made attempts to introduce reshaped reward functions and techniques of restricting action space to boost effective training. However, these algorithm needs careful designing in action space constraints and rewards to reluctantly obtain

effective training and executable gaits, while failing to out-strip zero-shot methods.

With world models exhibiting competence in heterogeneous downstream tasks [47–49], [14] employ the Dreamer world model in the real-world learning task. The model-based method, though a practical alternative, still suffers from the problem of deficient privileged knowledge. The model’s accuracy in featuring real-world information is also worth questioning in comparison with the simulation, as model-based methods are susceptible to pervasive model biases. The vulnerability of training also places the risk that convergence is not guaranteed facing the composition of model biases and compounding error.

III. METHODOLOGY

A. Preliminaries

We formulate the training process in the simulator as a Partially Observable Markov Decision Process (POMDP) as the environment cannot be fully observed. We define the MDP in the simulation as $\mathcal{M} = (\mathcal{S}, \mathcal{O}, \mathcal{A}, P, r, \gamma)$, where $\mathcal{S}, \mathcal{O}, \mathcal{A}$ denotes the state space, observation space, and action space respectively. $P(s_{t+1}|s_t, a_t)$ denotes the transition function, and the reward function is denoted as $r(s, a)$. γ denotes the discount factor. We define the privileged simulation parameters $c \in \mathcal{S} \setminus \mathcal{O}$ used to construct the simulation environment. Specifically, c contains the knowledge of the terrain distribution c_e (terrains are divided into 5 categories for feasibility) and robot-concerned parameters c_r (i.e. mass, restitution, motor strength). The goal of the RL method is to get the policy to maximize the expected discounted return:

$$\pi^* := \arg \max_{\pi} \mathbb{E}_{a_t \sim \pi(\cdot|o_t)} \left[\sum_{t=0}^{\infty} \gamma^t r(s_t, a_t) \right] \quad (1)$$

In the task of the lifelong policy adaptation, we need to find the optimal policy with the pretrained one in the real scene with the POMDP $\mathcal{M}^R = (\mathcal{S}^R, \mathcal{O}^R, \mathcal{A}^R, P^R, r^R, \gamma^R)$, where r^R is implicit without access. In the real-world setting, we are able to constantly collect trajectories but at an extremely low speed at least 1000 times slower than in the simulation.

In the later analysis, we take \mathcal{M} and \mathcal{M}^R to emblemize the training environment and the testing one.

B. Looping Sim and Real

We present our system for quadrupedal lifelong policy adaptation as **Looping Sim and Real** (LoopSR). The overview of LoopSR is depicted in Fig. 1. We draw on Proximal Policy Optimization (PPO) [50] to pretrain the policy in the IsaacGym environment following [3]. The policy is constructed following the state-of-the-art algorithm for quadrupedal locomotion [51–53], utilizing an Asymmetric Actor-Critic (AAC) architecture and expert motion data to enable robust sim-to-real transfer. Domain randomizations [6–8] are added to introduce a robust policy.

We used the collected trajectories with the environment parameters (privileged information & initial domain randomization range) during the training process to learn LoopSR-enc which projects the whole trajectory to the latent space

for relevant information. A multi-head decoder is designed to estimate the privileged information from the latent variable. In testing environments where the robot is deployed, the collected trajectory is encoded as the latent variable z^R . The estimated \hat{c} is the weighted sum of the retrieval results \hat{c}_{retr} referring to the training dataset of LoopSR-enc and the decoded results \hat{c}_{ml} , which is returned to IsaacGym environment to establish the simulation accordingly. Some techniques are taken to maintain stable training illustrated in Sec. III-D. The pseudocode 1 summarizes the whole pipeline.

Algorithm 1 The pipeline of LoopSR

Require: pretrain iterations n , start training iteration n_{start} , fusion ratio α , soft update ratio τ

- 1: Initialize policy π , LoopSR-enc f_θ and dataset $\mathcal{D} \leftarrow \emptyset$
- 2: Set the initial domain randomization (DR) range \mathcal{R} , and the continuous training DR range $\mathcal{R}' = \mathcal{R}/2$
- 3: Set $c^{curr} = (c_e^{curr}, c_r^{curr})$ as the average parameter
- 4:
- 5: // Pretrain policy in simulation
- 6: **for** $i = 1$ to n **do**
- 7: Rollout and store the trajectories, the relevant terrain distribution, and robot parameter $(\mathcal{T}, c_e, c_r) \rightarrow \mathcal{D}$
- 8: Update π through PPO Loss
- 9: **if** $i > n_{start}$ **then**
- 10: Update f_θ through Loss in (2) and (4)
- 11: Get reference latent space and simulation parameters $\mathcal{D}_z = f_\theta(\mathcal{T}), \mathcal{D}_c = \{c_e, c_r\}, \forall \mathcal{T}, c_e, c_r \in \mathcal{D}$
- 12:
- 13: // Lifelong policy adaptation
- 14: **repeat**
- 15: Collect testing environment trajectory \mathcal{T} with π
- 16: Get $z = q_\theta(\mathcal{T})$
- 17: Retrieve N nearest neighbours z_1, z_2, \dots, z_N of z in the latent space, and average the corresponding parameter c_1, c_2, \dots, c_N to get $\hat{c}_{retr} = [c'_e, c'_r]$
- 18: Get $\hat{c}_{ml} = [p_e(z), p_r(z)]$
- 19: Fuse predicted parameters $\hat{c} = \alpha \hat{c}_{retr} + (1 - \alpha) \hat{c}_{ml}$
- 20: Soft update $c_e^{curr} = \tau c_e^{curr} + (1 - \tau) \hat{c}_e$
- 21: Set $c_r^{curr} = \hat{c}_r$ with DR range \mathcal{R}'
- 22: Build the simulation according to c^{curr} in simulation and continue training π
- 23: **until forever**

C. Network Architecture

To the end of retaining the corresponding parameters of the testing environment, we design the network to cash in the latent space for knowledge distillation from real-world trajectories inspired by the advancements in representation learning methods [18, 19, 54]. The network architecture and its working flow are exhibited in Fig. 2.

Transformer-based Encoder. The key encoder, LoopSR-enc draws on Decision Transformer [55] or specifically follows [56] as the backbone while substituting the embedding of returns-to-go with the one of the next observation. LoopSR-enc $q_\theta(z|o_{1:n}, a_{1:n}, o_{2:n+1})$ receives the total trajectory without reward notation $\mathcal{T} = (o_{1:n}, a_{1:n}, o_{2:n+1})$ as

input. The output latent variable $z \in \mathbb{R}^{32}$ is the average pooling of the latent z_i from every timestep i and is modeled as a normal distribution following [19]. To support efficient learning [39, 57], we project z to an l_2 sphere to bound the latent space.

Autoencoder Architecture. To ensure that z captures enough features from the original trajectory, the training process is modeled as autoencoder(AE)-like with a decoder $q_\psi(\hat{o}_{t+1}|z, o_t, a_t)$ to reconstruct the new observations o_{t+1} based on the latent variable z , the observations o_t and the actions a_t inspired by [18]. We follow the common approach to use L2 distance as a supplant for the untractable log probability [18, 54, 58] of the next state prediction:

$$\mathcal{L} = \sum_{t=0}^n [o_{t+1} - q_\psi(q_\theta(\mathcal{T}), o_t, a_t)]^2, \forall \mathcal{T} \in \mathcal{B} \quad (2)$$

Contrastive Loss. To guide the model to implicitly discriminate different terrains, we apply the contrastive loss with the form of supervised InfoNCE loss similar to [23]. The loss is defined to maximize the inner product of z from the trajectories with the same terrain type label, whose theoretical background of maximizing the mutual information between positive samples and the latent representation is well-discussed in [22, 23].

$$\mathcal{L}_c = -\frac{1}{N} \sum_{i=1}^N \mathbf{1}_{c_e^i = c_e^j} \log \frac{\exp(z_i \cdot z_j)}{\sum_{j=1}^N \mathbf{1}_{i \neq j} \exp(z_i \cdot z_j)} \quad (3)$$

where N is the batch size.

Multi-head Decoder. We also design a multi-head decoder p_e and p_r to separately extract the terrain distribution and the robot proprioceptive parameters for disentanglement of different environment characteristics. We introduce c_e, c_r , and \mathcal{R} to represent the environment terrain distribution, robot parameter, and the range of the domain randomization in the training process. The losses are designed as follows:

$$\mathcal{L}_e = D_{KL}(p_e(z)||c_e), \quad \mathcal{L}_r = \frac{|p_r(z) - c_r|}{\mathcal{R}} \quad (4)$$

In Sec. IV-D, we conduct the ablation study to discuss the necessity of all loss terms.

It's noteworthy that z learns the manifold of simulation environments as LoopSR-enc and decoders are trained only on simulation data. This entails LoopSR with the potential capacity to find the best set of simulation parameters that generate a similar trajectory in the testing environment.

D. Implementation Details

Sampling-based Policy decomposition. Rather than collecting training data exclusively with the last pretrained policy, the dataset comprises trajectories sampled from different policy checkpoints. In this way, a sampling-based policy decomposition is inferred, ensuring stability when trajectories are collected from a constantly updating policy.

Soft Update. We implement the soft update of estimated environment parameters to avoid deleterious abrupt changes in terrain distribution. The terrain distribution is updated through $c^{curr} = \tau c^{curr} + (1 - \tau) \hat{c}$. τ is set to be 0.7. For the

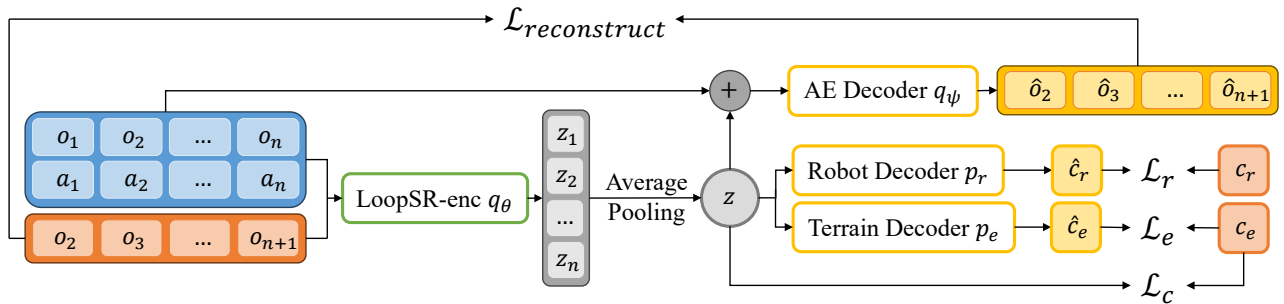


Fig. 2. Illustration of the core network architecture. The whole trajectory is input to a transformer backbone similar to [55], with output z derived from average pooling. The decoders are separately designed to disentangle different traits from the trajectory.

robot parameters, we half the domain randomization range to balance robustness and performance. Such a method has the adaptive ability to attune to the environment setting which is not in the initial reference dataset. The necessity of Soft update is illustrated in Sec. IV-D.

Retrieval Process. Regarding training safety, we use the retrieval method widely adopted in recommender systems [59] and the application of Large Language Models [60] to preclude drastically mistaken results in the face of out-of-distribution (o.o.d.) instances from learning-based methods. The final result is weighted as $c = \alpha \hat{c}_{retr} + (1 - \alpha) \hat{c}_{ml}$ with α in this work set to be 0.8.

E. Theoretical Analysis

We provide a theoretical analysis here to explain the effectiveness of LoopSR. With the No Free Lunch Theorem [9, 10] telling us a specific model may outstrip a general one, we demonstrate that the wide DR in policy training leads to suboptimal strategy in a specific environment. The discrepancy between optimal value functions in the training environment and the testing one is derived in Eq. 5.

$$\begin{aligned}
& |Q^*(s, a) - Q_R^*(s, a)| \\
&= \underbrace{\Delta r + \gamma \sum_{s', a'} P(s'|s, a) [\pi^* Q^* - \pi_R^* Q_R^*]}_{(i) \text{ total policy discrepancy}} \\
&+ \underbrace{\gamma \sum_{s', a'} P(s'|s, a) \pi_R^* Q_R^* - \gamma \sum_{s'', a''} P^R(s''|s, a) \pi_R^* Q_R^*}_{(ii) \text{ transition discrepancy}} \\
&\leq \frac{\Delta r}{1 - \gamma} + \frac{2\gamma r_{max}}{(1 - \gamma)^2} \epsilon_\pi + \frac{\gamma}{1 - \gamma} V_R^*(s') \epsilon_\rho
\end{aligned} \tag{5}$$

where Q^* and Q_R^* are optimal value functions in \mathcal{M} and \mathcal{M}^R respectively, and $V_R^*(s')$ as the optimal state value function on \mathcal{M}^R . Δr informs the discrepancy in reward functions, ϵ_π models the discrepancy caused by policy difference with detailed reasoning in [61], and ϵ_ρ denotes the discrepancy induced by the shift in state occupancy distribution. The discrepancies are detailed as follows:

$$\begin{aligned}
\Delta r &= r - r^R \\
\epsilon_\pi &= \sup_s D_{TV}(\pi^*(\cdot|o) || \pi_R^*(\cdot|o)) \\
\epsilon_\rho &= \mathbb{E}_s [D_{TV}(\rho(s) || \rho^R(s))]
\end{aligned}$$

In LoopSR, Δr is negligible as r is the sound approximate for r^R given the substantiated validity of r [3, 4, 15, 16]. For the second term, according to [61], ϵ_π will approach 0 with sufficient model capacity and iteration steps as π^* and π_R^* share the same input. For the last term, $\rho(s)$ is closely related to the innate state occupancy distribution (e.g. the state distribution of the stair terrain differs from the plain one). Parameter c can efficiently model such an error and mitigate it. To sum up, LoopSR can eliminate the discrepancy in Eq. 5 through effective modeling of each term, thus optimizing the policy performance.

IV. EXPERIMENTS

A. Sim-to-Sim Experiment

Overview. Although simulation settings cannot perfectly replicate real-world complexities, they offer a controlled environment for conducting statistical experiments, facilitating comparisons when direct real-world computation is impractical. We leverage IsaacGym [1] for training and simulation, which provides implementations of various terrains. The training code is developed based on [3].

The experiment consists of two primary phases. The first phase is pretraining in the training environment, where 4,096 robots are simulated across five distinct terrains (upward/downward slopes/stairs and flat ground), training in parallel for 30,000 iterations, with 24 simulation steps per iteration. The second phase involves data collection and continual training in a testing environment chosen from three terrains, each with three difficulty levels, defined by parameters of inclination, step height, and obstacle height, respectively (see Table I). Privileged knowledge is not accessed in the testing environment to simulate real-world conditions better. Each policy is trained on $1e5$ steps of collected data, equivalent to half an hour in a real-world experiment. During evaluations, robots are commanded to walk forward at a velocity of $v_x^{cmd} = 1.0m/s$ to assess their maximum performance. The reward functions follow [3] and are averaged across simulation steps. LoopSR takes out 100 sim-to-real loops for each terrain during simulation experiments.

Baselines. The baselines are defined as follows:

- **Expert** is a reference policy completely trained on the desired test environment.
- **Origin** is a reference policy without any refinement, representing a zero-shot sim-to-real workflow. It is

TABLE I: THE RESULT IN ISAACGYM SIMULATION CROSS DIFFERENT TERRAINS

Terrain	Difficulty	Expert	Origin	LoopSR(ours)	PPO	SAC	World Model
Stairs	0.122	1.3731±0.0002	1.2238±0.00189	1.3084±0.00062	1.2352±0.00003	0.2662±0.07617	0.1274±0.03480
	0.176	1.3519±0.0003	1.1874±0.00043	1.2522±0.00023	0.3523±0.00011	0.0386±0.00506	0.0619±0.01521
	0.23	1.2414±0.0354	0.7553±0.12505	1.1330±0.00813	0.5724±0.23479	0.0253±0.00024	0.0436±0.02800
Slope	0.24	1.4025±0.00001	1.3683±0.00003	1.3908±0.00001	1.3232±0.00006	0.1877±0.04915	0.2813±0.01686
	0.6	1.3478±0.00012	1.1968±0.00087	1.3417±0.00020	1.1754±0.00037	0.1539±0.05367	0.2222±0.02665
	0.9	1.1758±0.01412	0.5801±0.24676	1.0746±0.03184	0.5145±0.2649	0.0622±0.02096	0.1227±0.03877
Discrete	0.13	1.3519±0.00137	1.2202±0.01363	1.2648±0.00193	0.7723±0.01149	0.3354±0.05142	0.1607±0.04661
	0.19	1.1638±0.14744	0.9932±0.06514	1.0918±0.01214	0.2707±0.02512	0.0354±0.05214	0.1280±0.04706
	0.25	0.8681±0.26708	0.4056±0.21618	0.8379±0.19660	0.1151±0.02065	0.0138±0.04024	0.1768±0.01260

trained for the same number of timesteps as the combined pretraining and continual training steps.

- **PPO** is the vanilla PPO method without the privileged knowledge with a reward function the same as Origin, excluding privileged terms.
- **SAC** follows [11] with SAC used to pretrain and continual training. We modify the target velocity in the original reward function to $1.0m/s$ for testing.
- **World Model** indicates the model-based method in [14], with Dreamer [47] as the backbone.

Results. The simulation results are shown in Tab. I, where LoopSR achieves prominent enhancement and closely matches the performance of Expert, especially in challenging terrains like *Stairs* and *Discrete*. This outperformance over Origin confirms LoopSR’s success in continuous optimization. At the same time, direct real-world training approaches (PPO, SAC, World Model) mainly fail such an aim, typically owing to their fragility to the shift in state occupancy distribution. The reward curve concerning the sim-to-real loops is shown in Fig. 3, where each sim-to-real loop integrates simulated training of 500 iterations. We find out that LoopSR surpasses the performance bottleneck which troubles the original baseline.

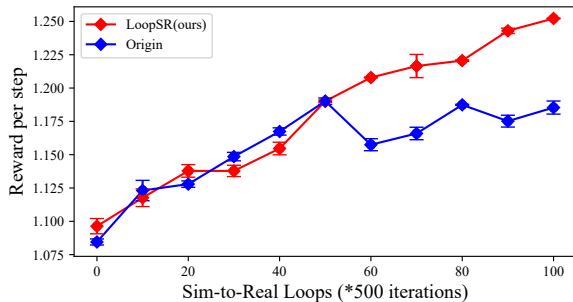


Fig. 3. Continual training curve compared with **Origin** baseline.

B. Sim-to-Real Evaluation

Overview. For real-world evaluations, we utilize the Uni-tree A1 robot [62] to facilitate real-world deployment. The pretraining process is identical to the sim-to-sim experiments, and the testing environment consists of diverse real-world terrains, as depicted in Fig. 4.

Data collected in the real world are transmitted to a host computer with a GTX 4090 GPU to execute the continual training. Trajectories are collected with a length of 4 seconds each. After each batch of 5 trajectories is collected, the agent



Fig. 4. Visualization of real-world application scenes.

is trained for an episode of 200 iterations in the simulation. Here, we only update the onboard policy after 10 episodes to simplify the data collection process. We demonstrate that this simplicity approximates the real workflow for the empirical consistency in simulation parameters predicted from trajectories collected by different policies.

The real-world observation includes proprioception $o_t \in \mathbb{R}^{45}$, obtained or estimated from the onboard sensors and IMU. The action $a_t \in \mathbb{R}^{12}$ specifies target joint positions converted to joint torques via a PD controller with stiffness and damping set to 28.0 and 0.7, respectively. The policy operates at 50 Hz.

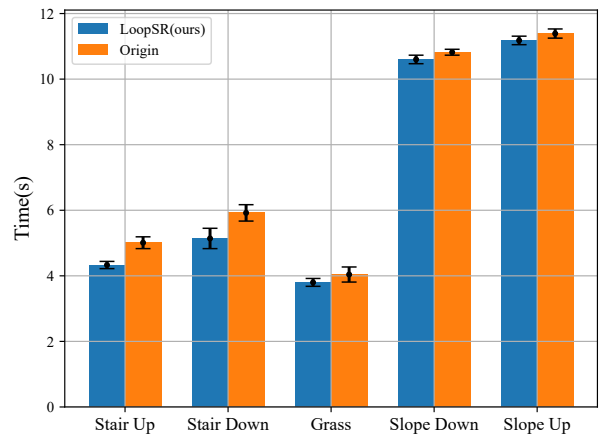


Fig. 5. Time cost to traverse certain paths on different terrains. ↓

We compare our method to Origin in Sec. IV-A to highlight the improvement. Each evaluation includes 10 trials to reduce stochasticity while obviating damage to robot hardware. The performance metrics include the time required to traverse through a specified path and the success rate in demanding terrains.

Results. The results in Fig. 5 and Tab. II demonstrate that LoopSR achieves superior performance across all tasks com-

TABLE II: THE SUCCESS RATE IN CHALLENGING TERRAINS.

	Stair Up	Stair Down	Pit
<i>LoopSR(Ours)</i>	100	100	90
<i>Origin</i>	70	90	80

pared with Origin, and ensures better safety during operation. The results indicate that LoopSR enhances locomotion policy capacity and fulfills the purpose of lifelong policy adaptation.

C. Empirical Study on Gaits

To further illustrate the effect of our method, we take the stair terrain as an example and analyze the gaits.

In the simulation, we visualize the robot’s contact phase of one foot in Fig. 6, showing that our method gradually reaches the periodical gait of the expert. At the same time, the baseline without refinement frequently missteps.

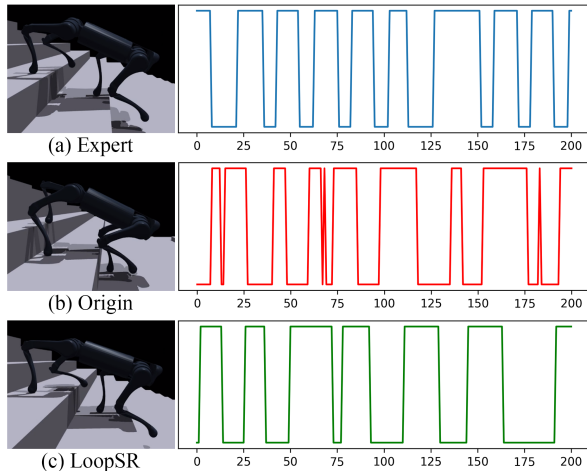


Fig. 6. Visualization of simulation gaits and contact phase.

In real-world experiments, We present snapshots of several jerky actions from Origin that triggered the safety module, along with corresponding gaits from the refined policy in Fig. 7. The baseline reacts violently to terrain changes, producing unstable motions and raising the robot in the air, which risks damaging the hardware. In comparison, refined policy smoothly adapts to such variations, guaranteeing safety in real-world applications.



Fig. 7. Comparison of motions from baseline Origin and LoopSR.

The dominance of our method in stair terrain proves that privileged knowledge, such as height fields and collisions, becomes crucial when facing challenging terrains, especially height-sensitive terrains.

D. Ablation Study

We conduct the ablation study to verify each component of LoopSR. To determine the importance of each loss, we test the accuracy of the variants in identifying different terrains and robot parameters. We also provide the policy without a soft update in training to validate its importance. The variants are designed as:

- **LSR-w/o-con** eliminates the constrastive loss with only the multihead predictor to learn the latent space.
- **LSR-w/o-AE** dismisses the reconstruction loss in the training process and depends on the constrastive loss to drive learning.
- **LSR-w/o-su** excludes the soft update in continual training. Results in Tab. III are the percentages of rewards from **LSR-w/o-su** to the rewards from **LSR**.

From Tab. III, **LSR** with all losses outperforms all counterparts to classify the terrains accurately. The comparable failure of **LSR-w/o-con** signifies the importance of the constrastive loss [53] in building a robust and interpretable latent space. The comparison between **LSR** and **LSR-w/o-AE** proves that the autoencoder structure is beneficial in extracting enough information from the trajectories. **LSR-w/o-su** drastically underperforms on demanding terrains, demonstrating the necessity of soft update.

TABLE III: ABLATION OF COMPONENTS. RESULTS IN PERCENTAGES.

Domain	LSR	LSR-w/o-con	LSR-w/o-AE	LSR-w/o-su
<i>Slope</i>	81.2	48.7	52.5	38.3
<i>Stair</i>	92.1	66.5	74.5	40.6
<i>Plain</i>	87.9	81.6	50.9	/
<i>Friction</i>	19.08	22.72	23.28	/
<i>Mass</i>	24.37	24.88	24.71	/

V. CONCLUSIONS AND LIMITATIONS

In summary, we propose a novel lifelong policy adaptation method named LoopSR based on looping data collection in real and continual training in the simulated reconstruction. The core of LoopSR is a transformer-based encoder that builds up an effective latent space from real-world trajectories for efficient retrieval and decoding. Autoencoder architecture and constrastive loss are implemented for generalizability and robustness. Decent techniques are employed to consolidate a comprehensive pipeline that exhibits extraordinary performance in both simulation and real-world experiments.

There are several limitations to address in future work. Further theoretical analysis is needed to better understand the contributions of the robot and environment to real-world dynamics, as self-cognition is crucial for human-like activities. Additionally, our method excludes visual perception. An ambitious future goal is to enable robots to reconstruct the real world in simulations using visual input and to learn new skills directly.

REFERENCES

- [1] V. Makoviychuk, L. Wawrzyniak, Y. Guo, M. Lu, K. Storey, M. Macklin, D. Hoeller, N. Rudin, A. Allshire, A. Handa, and G. State, “Isaac gym: High performance gpu-based physics simulation for robot learning,” *CoRR*, 2021.
- [2] E. Todorov, T. Erez, and Y. Tassa, “Mujoco: A physics engine for model-based control,” in *2012 IEEE/RSJ international conference on intelligent robots and systems*. IEEE, 2012, pp. 5026–5033.
- [3] N. Rudin, D. Hoeller, P. Reist, and M. Hutter, “Learning to walk in minutes using massively parallel deep reinforcement learning,” in *Conference on Robot Learning*. PMLR, 2022, pp. 91–100.
- [4] J. Lee, J. Hwangbo, L. Wellhausen, V. Koltun, and M. Hutter, “Learning quadrupedal locomotion over challenging terrain,” *Science robotics*, vol. 5, no. 47, p. eabc5986, 2020.
- [5] J. Tan, T. Zhang, E. Coumans, A. Iscen, Y. Bai, D. Hafner, S. Bohez, and V. Vanhoucke, “Sim-to-real: Learning agile locomotion for quadruped robots,” *arXiv preprint arXiv:1804.10332*, 2018.
- [6] J. Tobin, R. Fong, A. Ray, J. Schneider, W. Zaremba, and P. Abbeel, “Domain randomization for transferring deep neural networks from simulation to the real world,” in *2017 IEEE/RSJ international conference on intelligent robots and systems (IROS)*. IEEE, 2017, pp. 23–30.
- [7] X. B. Peng, M. Andrychowicz, W. Zaremba, and P. Abbeel, “Sim-to-real transfer of robotic control with dynamics randomization,” in *2018 IEEE international conference on robotics and automation (ICRA)*. IEEE, 2018, pp. 3803–3810.
- [8] Z. Xie, X. Da, M. van de Panne, B. Babich, and A. Garg, “Dynamics randomization revisited: A case study for quadrupedal locomotion,” in *2021 IEEE International Conference on Robotics and Automation (ICRA)*, 2021.
- [9] D. H. Wolpert and W. G. Macready, “No free lunch theorems for optimization,” *IEEE transactions on evolutionary computation*, vol. 1, no. 1, pp. 67–82, 1997.
- [10] D. H. Wolpert, “The lack of a priori distinctions between learning algorithms,” *Neural computation*, vol. 8, no. 7, pp. 1341–1390, 1996.
- [11] L. Smith, I. Kostrikov, and S. Levine, “Demonstrating a walk in the park: Learning to walk in 20 minutes with model-free reinforcement learning,” *Robotics: Science and Systems (RSS) Demo*, vol. 2, no. 3, p. 4, 2023.
- [12] L. Smith, J. C. Kew, X. B. Peng, S. Ha, J. Tan, and S. Levine, “Legged robots that keep on learning: Fine-tuning locomotion policies in the real world,” in *2022 International Conference on Robotics and Automation (ICRA)*. IEEE, 2022, pp. 1593–1599.
- [13] L. Smith, Y. Cao, and S. Levine, “Grow your limits: Continuous improvement with real-world rl for robotic locomotion,” in *2024 IEEE International Conference on Robotics and Automation (ICRA)*. IEEE, 2024, pp. 10 829–10 836.
- [14] P. Wu, A. Escontrela, D. Hafner, P. Abbeel, and K. Goldberg, “Daydreamer: World models for physical robot learning,” in *Conference on robot learning*. PMLR, 2023, pp. 2226–2240.
- [15] A. Agarwal, A. Kumar, J. Malik, and D. Pathak, “Legged locomotion in challenging terrains using ego-centric vision,” in *6th Annual Conference on Robot Learning*, 2022.
- [16] A. Kumar, Z. Fu, D. Pathak, and J. Malik, “Rma: Rapid motor adaptation for legged robots,” in *Robotics: Science and Systems*, 2021.
- [17] A. Vaswani, “Attention is all you need,” *Advances in Neural Information Processing Systems*, 2017.
- [18] R. Zhou, C.-X. Gao, Z. Zhang, and Y. Yu, “Generalizable task representation learning for offline meta-reinforcement learning with data limitations,” in *Proceedings of the AAAI Conference on Artificial Intelligence*, vol. 38, no. 15, 2024, pp. 17 132–17 140.
- [19] D. P. Kingma, “Auto-encoding variational bayes,” *arXiv preprint arXiv:1312.6114*, 2013.
- [20] F. Wang and H. Liu, “Understanding the behaviour of contrastive loss,” in *Proceedings of the IEEE/CVF Conference on Computer Vision and Pattern Recognition (CVPR)*, 2021.
- [21] X. Chen and K. He, “Exploring simple siamese representation learning,” in *Proceedings of the IEEE/CVF Conference on Computer Vision and Pattern Recognition (CVPR)*, 2021.
- [22] A. van den Oord, Y. Li, and O. Vinyals, “Representation learning with contrastive predictive coding,” 2019. [Online]. Available: <https://arxiv.org/abs/1807.03748>
- [23] P. Khosla, P. Teterwak, C. Wang, A. Sarna, Y. Tian, P. Isola, A. Maschinot, C. Liu, and D. Krishnan, “Supervised contrastive learning,” *Advances in neural information processing systems*, vol. 33, pp. 18 661–18 673, 2020.
- [24] B. Eysenbach, T. Zhang, S. Levine, and R. R. Salakhutdinov, “Contrastive learning as goal-conditioned reinforcement learning,” *Advances in Neural Information Processing Systems*, vol. 35, pp. 35 603–35 620, 2022.
- [25] M. Laskin, A. Srinivas, and P. Abbeel, “Curl: Contrastive unsupervised representations for reinforcement learning,” in *International conference on machine learning*. PMLR, 2020, pp. 5639–5650.
- [26] Y. Bengio, A. Courville, and P. Vincent, “Representation learning: A review and new perspectives,” *IEEE transactions on pattern analysis and machine intelligence*, vol. 35, no. 8, pp. 1798–1828, 2013.
- [27] W. Guo, J. Wang, and S. Wang, “Deep multimodal representation learning: A survey,” *Ieee Access*, vol. 7, pp. 63 373–63 394, 2019.
- [28] P. H. Le-Khac, G. Healy, and A. F. Smeaton, “Contrastive representation learning: A framework and review,” *Ieee Access*, vol. 8, pp. 193 907–193 934, 2020.
- [29] T. De Bruin, J. Kober, K. Tuyls, and R. Babuška,

- “Integrating state representation learning into deep reinforcement learning,” *IEEE Robotics and Automation Letters*, vol. 3, no. 3, pp. 1394–1401, 2018.
- [30] S. Park, T. Kreiman, and S. Levine, “Foundation policies with hilbert representations,” *arXiv preprint arXiv:2402.15567*, 2024.
- [31] A. Stooke, K. Lee, P. Abbeel, and M. Laskin, “Decoupling representation learning from reinforcement learning,” in *International conference on machine learning*. PMLR, 2021, pp. 9870–9879.
- [32] S. Nair, A. Rajeswaran, V. Kumar, C. Finn, and A. Gupta, “R3m: A universal visual representation for robot manipulation,” *arXiv preprint arXiv:2203.12601*, 2022.
- [33] K. Frans, S. Park, P. Abbeel, and S. Levine, “Unsupervised zero-shot reinforcement learning via functional reward encodings,” in *Forty-first International Conference on Machine Learning*, 2024.
- [34] Y. J. Ma, S. Sodhani, D. Jayaraman, O. Bastani, V. Kumar, and A. Zhang, “Vip: Towards universal visual reward and representation via value-implicit pre-training,” *arXiv preprint arXiv:2210.00030*, 2022.
- [35] A. Barreto, W. Dabney, R. Munos, J. J. Hunt, T. Schaul, H. P. van Hasselt, and D. Silver, “Successor features for transfer in reinforcement learning,” *Advances in neural information processing systems*, vol. 30, 2017.
- [36] C. Devin, A. Gupta, T. Darrell, P. Abbeel, and S. Levine, “Learning modular neural network policies for multi-task and multi-robot transfer,” in *2017 IEEE international conference on robotics and automation (ICRA)*. IEEE, 2017, pp. 2169–2176.
- [37] H. Ma, Z. Ren, B. Dai, and N. Li, “Skill transfer and discovery for sim-to-real learning: A representation-based viewpoint,” *arXiv preprint arXiv:2404.05051*, 2024.
- [38] G. B. Margolis and P. Agrawal, “Walk these ways: Tuning robot control for generalization with multiplicity of behavior,” in *Conference on Robot Learning*. PMLR, 2023, pp. 22–31.
- [39] J. Wu, Y. Xue, and C. Qi, “Learning multiple gaits within latent space for quadruped robots,” *arXiv preprint arXiv:2308.03014*, 2023.
- [40] A. Y. Ng, D. Harada, and S. Russell, “Policy invariance under reward transformations: Theory and application to reward shaping,” in *Icml*, vol. 99, 1999, pp. 278–287.
- [41] Z. Zhu, K. Lin, A. K. Jain, and J. Zhou, “Transfer learning in deep reinforcement learning: A survey,” *IEEE Transactions on Pattern Analysis and Machine Intelligence*, 2023.
- [42] D. Abel, A. Barreto, B. Van Roy, D. Precup, H. P. van Hasselt, and S. Singh, “A definition of continual reinforcement learning,” *Advances in Neural Information Processing Systems*, vol. 36, 2024.
- [43] D. Isele and A. Cosgun, “Selective experience replay for lifelong learning,” in *Proceedings of the AAAI Conference on Artificial Intelligence*, vol. 32, no. 1, 2018.
- [44] C. Kaplanis, C. Clopath, and M. Shanahan, “Continual reinforcement learning with multi-timescale replay,” *arXiv preprint arXiv:2004.07530*, 2020.
- [45] H. Ahn, J. Hyeon, Y. Oh, B. Hwang, and T. Moon, “Reset & distill: A recipe for overcoming negative transfer in continual reinforcement learning,” *arXiv preprint arXiv:2403.05066*, 2024.
- [46] M. Wolczyk, M. Zając, R. Pascanu, Ł. Kuciński, and P. Miłoś, “Disentangling transfer in continual reinforcement learning,” *Advances in Neural Information Processing Systems*, vol. 35, pp. 6304–6317, 2022.
- [47] D. Hafner, T. Lillicrap, J. Ba, and M. Norouzi, “Dream to control: Learning behaviors by latent imagination,” in *International Conference on Learning Representations*, 2019.
- [48] D. Hafner, T. P. Lillicrap, M. Norouzi, and J. Ba, “Mastering atari with discrete world models,” in *International Conference on Learning Representations*, 2020.
- [49] F. Ebert, C. Finn, S. Dasari, A. Xie, A. Lee, and S. Levine, “Visual foresight: Model-based deep reinforcement learning for vision-based robotic control,” *arXiv preprint arXiv:1812.00568*, 2018.
- [50] J. Schulman, F. Wolski, P. Dhariwal, A. Radford, and O. Klimov, “Proximal policy optimization algorithms,” *CoRR*, 2017.
- [51] I. M. A. Nahrendra, B. Yu, and H. Myung, “Dreamwaq: Learning robust quadrupedal locomotion with implicit terrain imagination via deep reinforcement learning,” in *2023 IEEE International Conference on Robotics and Automation (ICRA)*. IEEE, 2023, pp. 5078–5084.
- [52] J. Wu, G. Xin, C. Qi, and Y. Xue, “Learning robust and agile legged locomotion using adversarial motion priors,” *IEEE Robotics and Automation Letters*, 2023.
- [53] A. Escontrela, X. B. Peng, W. Yu, T. Zhang, A. Iscen, K. Goldberg, and P. Abbeel, “Adversarial motion priors make good substitutes for complex reward functions,” in *2022 IEEE/RSJ International Conference on Intelligent Robots and Systems (IROS)*. IEEE, 2022, pp. 25–32.
- [54] J. Chung, K. Kastner, L. Dinh, K. Goel, A. C. Courville, and Y. Bengio, “A recurrent latent variable model for sequential data,” *Advances in neural information processing systems*, vol. 28, 2015.
- [55] L. Chen, K. Lu, A. Rajeswaran, K. Lee, A. Grover, M. Laskin, P. Abbeel, A. Srinivas, and I. Mordatch, “Decision transformer: Reinforcement learning via sequence modeling,” *Advances in neural information processing systems*, vol. 34, pp. 15 084–15 097, 2021.
- [56] A. Radford, “Improving language understanding by generative pre-training,” https://cdn.openai.com/research-covers/language-unsupervised/language_understanding_paper.pdf, 2018.
- [57] X. B. Peng, Y. Guo, L. Halper, S. Levine, and S. Fidler, “Ase: large-scale reusable adversarial skill embeddings for physically simulated characters,” *ACM Transactions on Graphics*, vol. 41, no. 4, p. 1–17,

July 2022. [Online]. Available: <http://dx.doi.org/10.1145/3528223.3530110>

- [58] M. Babaeizadeh, C. Finn, D. Erhan, R. H. Campbell, and S. Levine, "Stochastic variational video prediction," in *International Conference on Learning Representations*, 2018.
- [59] J. Huang, J. Chen, J. Lin, J. Qin, Z. Feng, W. Zhang, and Y. Yu, "A comprehensive survey on retrieval methods in recommender systems," *arXiv preprint arXiv:2407.21022*, 2024.
- [60] Y. Gao, Y. Xiong, X. Gao, K. Jia, J. Pan, Y. Bi, Y. Dai, J. Sun, and H. Wang, "Retrieval-augmented generation for large language models: A survey," *arXiv preprint arXiv:2312.10997*, 2023.
- [61] H. He, P. Wu, C. Bai, H. Lai, L. Wang, L. Pan, X. Hu, and W. Zhang, "Bridging the sim-to-real gap from the information bottleneck perspective," in *8th Annual Conference on Robot Learning*, 2024. [Online]. Available: <https://openreview.net/forum?id=Bq4XOaU4sV>
- [62] Unitree, "Unitree robotics," <https://www.unitree.com/>, 2022.